

A Simple Algorithm for Exact Multinomial Tests^{*}

Johannes Resin

Heidelberg Institute for Theoretical Studies, Heidelberg, Germany
Karlsruhe Institute of Technology, Karlsruhe, Germany
e-mail: johannes.resin@h-its.org

Abstract: This work proposes a new method for computing acceptance regions of exact multinomial tests. From this an algorithm is derived, which finds exact p -values for tests of simple multinomial hypotheses. Using concepts from discrete convex analysis, the method is proven to be exact for various popular test statistics, including Pearson’s chi-square and the log-likelihood ratio. The proposed algorithm improves greatly on the naive approach using full enumeration of the sample space. However, its use is limited to multinomial distributions with a small number of categories, as the runtime grows exponentially in the number of possible outcomes.

The method is applied in a simulation study and uses of multinomial tests in forecast evaluation are outlined. Additionally, properties of a test statistic using probability ordering, referred to as the “exact multinomial test” by some authors, are investigated and discussed. The algorithm is implemented in the accompanying R package `ExactMultinom`.

Keywords and phrases: Acceptance regions, asymptotic approximation, forecast evaluation, goodness-of-fit test, hypothesis testing, log-likelihood ratio statistic, multinomial distribution, Pearson’s chi-square statistic, probability mass statistic, power, R software.

1. Introduction

Multinomial goodness-of-fit tests feature prominently in the statistical literature and a wide range of applications. Tests relying on asymptotics have been available for a long time and have been rigorously studied all through the 20th century. The use of various test statistics has been investigated with Pearson’s chi-square and the log-likelihood ratio statistic being vital examples. These statistics are members of the general family of power divergence statistics (Cressie and Read, 1984). With the widespread availability of computing power, Monte Carlo simulations and exact methods have also gained popularity.

As regards exact tests of a simple null hypothesis against an unspecified alternative, Tate and Hyer (1973) and Kotze and Gokhale (1980) used the “exact multinomial test”, which orders samples by probability to assess the accuracy of asymptotic tests. In the words of Cressie and Read (1989), this “has provided much confusion and contention in the literature”. In accordance with Gibbons

^{*}This work has been supported by the Klaus Tschira Foundation. I want to thank Tilmann Gneiting, Alexander Jordan and Sebastian Lerch for helpful comments, discussions and continued encouragement.

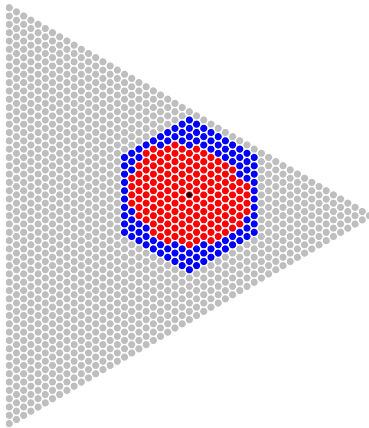


FIG 1. An acceptance region (red) at level $\alpha = 0.05$ for the null $\pi = (\frac{2}{10}, \frac{5}{10}, \frac{3}{10})$ and samples of size $n = 50$ with $m = 3$ categories. Only the points within the ball (blue) around the expectation (black point) have to be considered to find this acceptance region.

and Pratt (1975) and Radlow and Alf (1975), they conclude that the asymptotic fit of a test should be assessed using the appropriate exact test based on the test statistic in question. Nevertheless, the exact multinomial test is intuitively appealing and, as Kotze and Gokhale (1980) put it, “[i]n the absence of [...] a specific alternative, it is reasonable to assume that outcomes with smaller probabilities under the null hypothesis offer a stronger evidence for its rejection and should belong to the critical region”. In Section 2, an asymptotic chi-square approximation to the exact multinomial test is derived and an exemplary comparison of popular test statistics in terms of power is provided.

Regardless of the test statistic used, calculating an exact p -value by fully enumerating the sample space is computationally challenging, as the test statistic and the probability mass function have to be evaluated at every possible sample of which there are $\binom{n+m-1}{m-1} = \mathcal{O}(n^{m-1})$ for samples of size n with m categories. An improvement on this method has been proposed by Bejerano, Friedman and Tishby (2004) and other, more elaborate approaches exist (see for example Baglivo, Olivier and Pagano, 1992; Hirji, 1997; Keich and Nagarajan, 2006). In this work, a new approach to exact multinomial tests is investigated.

The key observation underlying the proposed algorithm is that acceptance regions at arbitrary levels contain relatively few points, which are located in a neighborhood of the expected value under the null hypothesis as illustrated in Figure 1. An acceptance region can be found by iteratively evaluating points within a ball of increasing radius around the expected value (w.r.t. the Manhattan distance). From this procedure an algorithm for computing exact p -values is derived by finding the probability mass of the smallest acceptance region that does not contain an observation. If p -values below an arbitrary threshold are not calculated exactly, the runtime of the algorithm is guaranteed to be asymp-

totically faster than the approach using full enumeration as the diameter of any acceptance region essentially grows at a rate proportional to the square root of the sample size. This is detailed and proven to work for various popular test statistics in Section 3.

Furthermore, the algorithm is illustrated to work well in applications detailed in Section 4. In particular, the algorithm's runtime is compared to the full enumeration method in a simulation study and the resulting p -values are used to assess the fit of asymptotic chi-square approximations and investigate differences between several test statistics. As a further application, the use of multinomial tests to quantify the gravity of discrepancies in forecast probabilities and outcome frequencies within the so-called calibration simplex (Wilks, 2013) is outlined and justified.

The R programming language (R Core Team, 2020) has been used for all calculations throughout this work. An implementation of the proposed method is provided within the R package `ExactMultinom` available at the CRAN package repository (<https://cran.r-project.org/>).

2. A Brief Review on Testing a Simple Multinomial Hypothesis

Consider a multinomial experiment $X = (X_1, \dots, X_m)$ summarizing $n \in \mathbb{N}$ i.i.d. trials with $m \in \mathbb{N}$ possible outcomes. Let

$$\Delta_{m-1} := \{p \in [0, 1]^m \mid p_1 + \dots + p_m = 1\}$$

denote the *unit* $(m-1)$ -simplex or *probability simplex* and

$$\Delta_{m-1}^n = \{x \in \mathbb{N}_0^m \mid x_1 + \dots + x_m = n\}$$

the *regular discrete* $(m-1)$ -simplex. The distribution of X is characterized by a parameter $p = (p_1, \dots, p_m) \in \Delta_{m-1}$ encoding the occurrence probabilities of the outcomes on any trial, or $X \sim \mathcal{M}_m(n, p)$ for short. The multinomial distribution $\mathcal{M}_m(n, p)$ is fully described by the probability mass function (pmf)

$$f_{n,p}: \Delta_{m-1}^n \rightarrow [0, 1], x \mapsto n! \prod_{j=1}^m \frac{p_j^{x_j}}{x_j!}.$$

Suppose that the true parameter p is unknown. Consider the simple null hypothesis $p = \pi$ for some $\pi \in \Delta_{m-1}$. The agreement of a realization $x \in \Delta_{m-1}^n$ of X with the null hypothesis is typically quantified by means of a test statistic $T: \Delta_{m-1}^n \times \Delta_{m-1} \rightarrow \mathbb{R}$. Given such a test statistic T and presuming from now on that w.l.o.g. high values of $T(x, \pi)$ indicate 'extreme' observations under the null distribution \mathbb{P}_π , the p -value of x is defined as the probability

$$p_T(x, \pi) := \mathbb{P}_\pi(T(X, \pi) \geq T(x, \pi)) \quad (1)$$

of observing an observation that is at least as extreme under the null hypothesis.

The family of power divergence statistics introduced by Cressie and Read (1984) offers a variety of test statistics for multinomial goodness-of-fit tests. It is defined as

$$T^\lambda(x, \pi) := \frac{2}{\lambda(\lambda+1)} \sum_{j=1}^m x_j \left(\left(\frac{x_j}{n\pi_j} \right)^\lambda - 1 \right) \text{ for } \lambda \in \mathbb{R} \setminus \{-1, 0\} \quad (2)$$

and as the pointwise limit in (2) for $\lambda \in \{-1, 0\}$. Notably, this includes Pearson's chi-square statistic

$$T^{\chi^2}(x, \pi) := \sum_{j=1}^m \frac{(x_j - n\pi_j)^2}{n\pi_j} = \sum_{j=1}^m \frac{x_j^2}{n\pi_j} - n = T^1(x, \pi)$$

as well as the log-likelihood ratio (or G-test) statistic

$$T^G(x, \pi) := 2 \log \frac{f_{n, \frac{x}{n}}(x)}{f_{n, \pi}(x)} = 2 \sum_{j=1}^m x_j \log \frac{x_j}{n\pi_j} = T^0(x, \pi).$$

Under a null hypothesis with $\pi_i > 0$ for all $i = 1, \dots, m$, every power divergence statistic is asymptotically chi-square distributed with $m - 1$ degrees of freedom.

A natural test statistic arises if an 'extreme' observation is simply understood to mean an unlikely one, that is, if the pmf itself is used as test statistic. In what follows, a strictly decreasing transformation of the pmf is used instead, which ensures that large values of the test statistic indicate extreme observations. Furthermore, this strictly decreasing transformation is chosen such that the resulting test statistic is asymptotically chi-square distributed.

To this end, let Γ denote the Gamma function and

$$\bar{f}_{n,p} : \{x \in \mathbb{R}_{\geq 0}^m \mid x_1 + \dots + x_m = n\} \rightarrow \mathbb{R}, x \mapsto \Gamma(n+1) \prod_{j=1}^m \frac{p_j^{x_j}}{\Gamma(x_j+1)}$$

the continuous extension of the pmf $f_{n,p}$ to the convex hull of the discrete simplex Δ_{m-1}^n and define the probability mass test statistic as

$$T^{\mathbb{P}}(x, \pi) := -2 \log \frac{f_{n,\pi}(x)}{\bar{f}_{n,\pi}(n\pi)}.$$

Obviously, the choice of strictly decreasing transformation does not affect the (exact) p -value given by (1) for $T = T^{\mathbb{P}}$. The following theorem gives rise to an asymptotic approximation of p -values derived from the probability mass test statistic, which has not been studied previously. In the simulation study of Section 4, the fit of this approximation is assessed empirically using exact p -values calculated with the new method for samples of size $n = 100$ with $m = 5$ categories.

Theorem 1. *If $X \sim \mathcal{M}_m(n, \pi)$ follows a multinomial distribution with $n \in \mathbb{N}$ and $\pi \in \Delta_{m-1}$ such that $\pi_j > 0$ for $j = 1, \dots, m$, then $T^{\mathbb{P}}(X, \pi)$ converges in distribution to a chi-square distribution χ_{m-1}^2 with $m - 1$ degrees of freedom as $n \rightarrow \infty$.*

Proof. By Lemma 7 (in Appendix A), the difference between the log-likelihood ratio and the probability mass statistic is

$$T^{\mathbb{P}}(X, \pi) - T^G(X, \pi) = \sum_{j=1}^m \left(\log \frac{X_j}{n\pi_j} + \mathcal{O}(1/X_j) - \mathcal{O}(1/n) \right).$$

Clearly, the bounded terms converge to zero in probability and the $\log \frac{X_j}{n\pi_j}$ terms converge to zero in probability by the continuous mapping theorem. Hence, the probability mass statistic has the same asymptotic distribution as the log-likelihood ratio statistic. \square

In what follows, the focus is on the chi-square, log-likelihood ratio and probability mass statistics.

2.1. Acceptance Regions

As outlined in the introduction, acceptance regions are of major importance to the idea pursued in this work. Given a test statistic T , the *acceptance region at level $\alpha > 0$* is defined as

$$A_{n,\pi}^T(\alpha) := \{x \in \Delta_{m-1}^n \mid p_T(x, \pi) \geq \alpha\}.$$

Equivalently, the acceptance region can be written as the *sublevel set* of $T(\cdot, \pi)$ at any $(1-\alpha)$ -quantile $t_{1-\alpha}$ of $T(X, \pi)$ under the null hypothesis $X \sim \mathcal{M}_m(n, \pi)$, i.e.,

$$A_{n,\pi}^T(\alpha) = \{x \in \Delta_{m-1}^n : T(x, \pi) \leq t_{1-\alpha}\}.$$

By construction, the probability mass test statistic often yields a smallest acceptance region, because it assigns the samples with largest probabilities to the acceptance region. This is the case precisely if $\mathbb{P}_\pi(X \in A_{n,\pi}^{T^{\mathbb{P}}}(\alpha)) - (1-\alpha) < \min_{x \in A_{n,\pi}^{T^{\mathbb{P}}}(\alpha)} \mathbb{P}_\pi(X = x)$. If tests are randomized to ensure equal level and size of the test, this property can be refined to yield an optimality property of the probability mass test's critical function. Figure 2 illustrates acceptance regions for different test statistics.

In Section 3, it will be shown that acceptance regions of the chi-square, log-likelihood ratio and probability mass test statistic all grow at a rate $\mathcal{O}(n^{\frac{m-1}{2}})$, as their diameter grows at a rate $\mathcal{O}(\sqrt{n})$ if $\alpha > 0$ is fixed, see Proposition 6.

2.2. Power and Bias

The power function of a test T of the null hypothesis $p = \pi$ at level α is

$$\Delta_{m-1} \rightarrow [0, 1], p \mapsto 1 - \mathbb{P}_p(T(X) \in A_{n,\pi}^T(\alpha)),$$

which is the probability of rejecting the null hypothesis at level α if the true parameter is p . The *size* of a test is its power at $p = \pi$. A test T is said to be *unbiased* (for the null $p = \pi$ at level α) if its power is minimized at $p = \pi$.

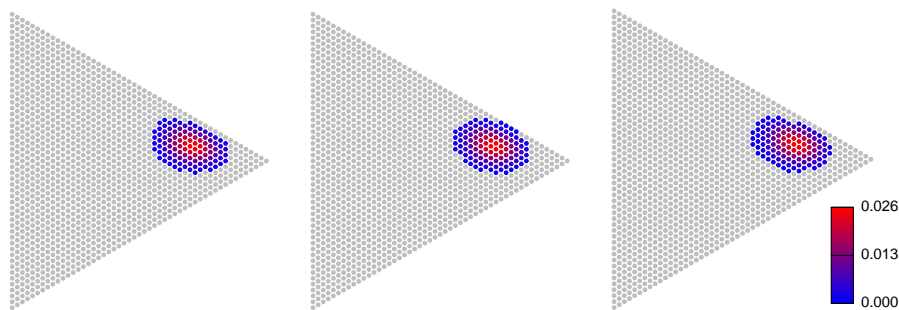


FIG 2. Acceptance regions of probability mass (left), chi-square (center) and log-likelihood ratio (right) statistics at level $\alpha = 0.05$ for $n = 50$ and $\pi = (\frac{1}{10}, \frac{7}{10}, \frac{2}{10})$. The regions contain 108, 111 and 111 points, respectively (left to right). The tests are of size 0.0495, 0.0492 and 0.0481, respectively. The color gradient represents (null) probabilities within the regions.

In case of the uniform null hypothesis, i.e., $\pi = (\frac{1}{m}, \dots, \frac{1}{m})$, [Cohen and Sackrowitz \(1975, Theorem 2.1\)](#) proved that the power function increases away from $p = \pi$ for tests statistics of the form

$$T(x) = \sum_{j=1}^m h(x_j)$$

if h is a convex function. They concluded that tests based on the chi-square and the log-likelihood ratio test statistic are unbiased for the uniform null hypothesis. As a corollary to their theorem, it shall be noted that this also applies to the probability mass test statistic.

Corollary 2 (to [Cohen and Sackrowitz, 1975, Theorem 2.1](#)). *The probability mass test is unbiased for the uniform null hypothesis $p = \pi = (\frac{1}{m}, \dots, \frac{1}{m})$.*

Proof. Since the probability mass statistic can be written as

$$T^{\mathbb{P}}(x, \pi) = 2 \sum_{j=1}^m \log \Gamma(x_j + 1) - x_j \log \pi_j - \log \frac{\Gamma(n\pi_j + 1)}{\pi_j^{n\pi_j}},$$

this is an immediate consequence of the fact that the Gamma function is logarithmically convex on the positive real numbers, which is part of a characterization given by the Bohr-Mollerup theorem ([Beals and Wong, 2010, Theorem 2.4.2](#)). \square

Many authors (e.g., [West and Kempthorne, 1972](#); [Cressie and Read, 1984](#); [Wakimoto, Odaka and Kang, 1987](#); [Pérez and Pardo, 2003](#)) have conducted small sample studies to investigate the power of chi-square, log-likelihood ratio and other tests. In conducting these studies π, n and α need to be chosen, all of which influence the resulting power function. Furthermore, it is frequently

infeasible to assess the power function across all alternatives and so alternatives of interest need to be picked.

Therefore, most of these studies focused on the case of the uniform null hypothesis. In this case, the chi-square test has greater power for alternatives that assign a large proportion of the probability mass to relatively few classes, whereas the log-likelihood ratio test has greater power for alternatives that assign considerable probability mass to many classes (see also [Koehler and Larntz, 1980](#)).

In the ternary case, that is, if $m = 3$, comparisons on the full probability simplex are visually accessible. Figure 3 illustrates, which of the three test statistics yields the highest and lowest power across the full ternary probability simplex. As the actual size of the test varies with the choice of the test statistic due to the actual size of a test frequently being smaller than the level α , the resulting power functions are difficult to compare directly.

To account for this, the tests are randomized to ensure that their respective size matches the level. For a test T and level α , let $s_{n,\pi}(T, \alpha) = 1 - \mathbb{P}_\pi(T(X) \in A_{n,\pi}^T(\alpha))$ denote the actual size of the test. The *critical function*

$$\phi: \Delta_{m-1}^n \rightarrow [0, 1], x \mapsto \begin{cases} 0, & \text{if } T(x, \pi) < t_{1-\alpha}, \\ \frac{\alpha - s_{n,\pi}(T, \alpha)}{\mathbb{P}_\pi(T(X) = t_{1-\alpha})}, & \text{if } T(x, \pi) = t_{1-\alpha}, \\ 1, & \text{if } T(x, \pi) > t_{1-\alpha}, \end{cases}$$

defines a randomized test¹, which rejects the null hypothesis with probability $\phi(x)$ if x is observed. The power function of the randomized version of a test T at level α is

$$p \mapsto \sum_{x \in \Delta_{m-1}^n} \phi(x) \mathbb{P}_p(X = x) = 1 - \sum_{x \in A_{n,\pi}^T(\alpha)} (1 - \phi(x)) \mathbb{P}_p(X = x).$$

With this, the probability mass test minimizes the acceptance region in the sense that it minimizes the sum

$$\sum_{x \in \Delta_{m-1}^n} (1 - \phi(x))$$

across all randomized tests ϕ with $\sum_x \phi(x) f_{n,\pi}(x) = \alpha$.

Figure 3 suggests that the probability mass test and the log-likelihood ratio test for the uniform null hypothesis are the same. However, this is not generally true as for other choices of α (e.g., $\alpha = 0.13$, for which coincidentally the probability mass statistic yields the same acceptance region as the chi-square statistic) the acceptance regions differ and so do the power functions.

Figure 4 quantitatively compares powers along alternatives of the form

$$p(q, i) = (\tilde{q}\pi_1, \dots, \tilde{q}\pi_{i-1}, q, \tilde{q}\pi_{i+1}, \dots, \tilde{q}\pi_m) \in \Delta_m \text{ with } \tilde{q} = \frac{1 - q}{1 - \pi_i}$$

¹Randomized tests like this traditionally arise in the theory of uniformly most powerful tests, see for example [Lehmann and Romano \(2005, Chapter 3\)](#).

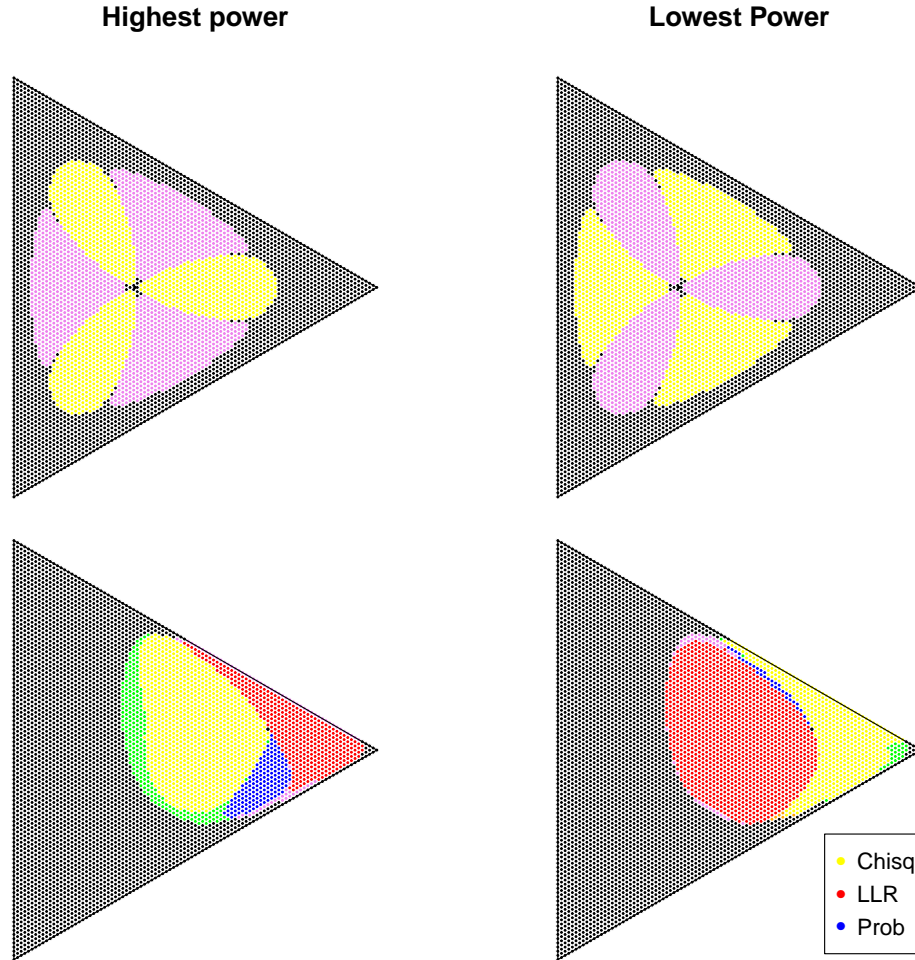


FIG 3. Ternary plots indicating the test statistic with the highest power (left) and lowest power (right) for the uniform null hypothesis $\pi = (\frac{1}{3}, \frac{1}{3}, \frac{1}{3})$ (top) and $\pi = (\frac{1}{10}, \frac{7}{10}, \frac{2}{10})$ (bottom) for $n = 50$ and randomized tests of size $\alpha = 0.05$. Mixtures of colors indicate nearly equal powers (difference ≤ 0.0001). For example, violet indicates nearly equal powers of the log-likelihood ratio (LLR) and probability mass (Prob) statistic. Black indicates areas where all powers are nearly equal.

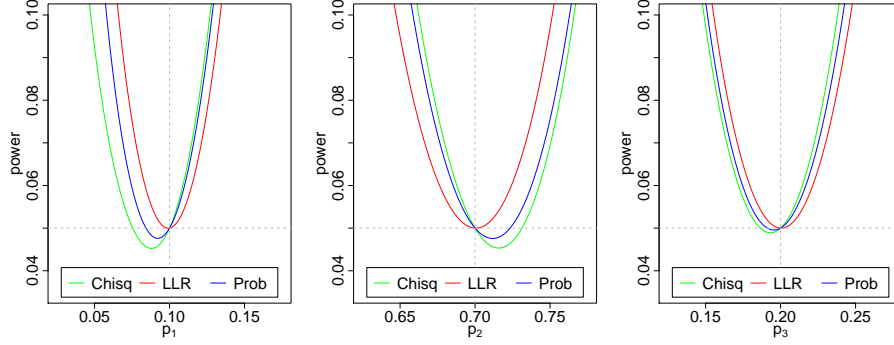


FIG 4. Power functions along alternatives given by $p(p_i, i)$, $i = 1, 2, 3$ for randomized tests of size $\alpha = 0.05$ of null hypothesis $\pi = (\frac{1}{10}, \frac{7}{10}, \frac{2}{10})$ and sample size $n = 50$.

for $i = 1, \dots, m$ and $q \in [0, 1]$. This yields parametrizations of the lines through π and a corner of the probability simplex. The figures illustrate that in the case $n = 50$, $\pi = (\frac{1}{10}, \frac{7}{10}, \frac{2}{10})$ and $\alpha = 0.05$, the log-likelihood ratio test, arguably, does not show any visible bias, whereas the chi-square test shows the most bias. The power function of the probability mass test lies in between the other power functions across most of the probability simplex and so the probability mass test might serve as a good compromise in terms of power.

3. Exact p -Values via Acceptance Regions

Throughout this section, T is some test statistic and $m, n \in \mathbb{N}$ and $\pi \in \Delta_{m-1}$ are considered fixed. To ease notation, the subscripts in the pmf of the null distribution are omitted, i.e., $f = f_{n, \pi}$ and the test statistic T is considered as a function on the sample space only, i.e., $T(\cdot) = T(\cdot, \pi)$. Let

$$d: \mathbb{R}^m \times \mathbb{R}^m \rightarrow \mathbb{R}_{\geq 0}, (x, y) \mapsto \frac{1}{2} \|x - y\|_1 = \frac{1}{2} \sum_j |x_j - y_j|$$

be a rescaled version of the *Manhattan distance* and

$$B_r(y) = \{x \in \Delta_{m-1}^n \mid d(x, y) \leq r\}$$

the ball with radius $r \in \mathbb{N}$ and center $y \in \Delta_{m-1}^n$. Furthermore, $e_i = (\delta_{ij})_{j=1}^m$ denotes the i -th vector of the standard basis of \mathbb{R}^m .

3.1. Finding acceptance regions using discrete convex analysis

As alluded to in the introduction, an acceptance region $A = A_{n, \pi}^T(\alpha)$ for $\alpha \in (0, 1)$ can be found without enumerating all points of the sample space Δ_{m-1}^n ,

but only considering points in some ball around the expected value for many test statistics. Specifically, if T is *weakly quasi M-convex*, that is, for all distinct $x, y \in \Delta_{m-1}^n$ there exist indices $i, j \in \{1, \dots, m\}$ such that $x_i > y_i, x_j < y_j$ and

$$T(x - e_i + e_j) \leq T(x) \quad \text{or} \quad T(y + e_i - e_j) \leq T(y),$$

the following theorem holds.

Theorem 3. *Let T be weakly quasi M-convex. Let $y \in \Delta_{m-1}^n$ and $r \in \mathbb{N}$ such that $\sum_{x \in B_r(y)} f(x) \geq 1 - \alpha$ for some $\alpha \in (0, 1)$. If there exists a subset $A \subset B_{r-1}(y)$ of the form $A = \{x \in B_r(y) \mid T(x) \leq t\}$ such that $\sum_{x \in A} f(x) \geq 1 - \alpha$, then the smallest such subset is the acceptance region $A_{n,\pi}^T(\alpha)$.*

Hence, an acceptance region can be found by iteratively enumerating a ball of increasing radius with arbitrary center until a sublevel set with enough probability mass is found and this sublevel set remains unchanged upon further increasing the ball. This was illustrated in the introduction, see Figure 1 for an acceptance region of the probability mass statistic $T = T^{\mathbb{P}}$.

The following proposition ensures that this approach can be applied to the chi-square, log-likelihood ratio and probability mass test statistics.

Proposition 4.

- a) *The probability mass test statistic $T^{\mathbb{P}}$ is weakly quasi M-convex.*
- b) *The power divergence test statistic T^λ is weakly quasi M-convex if $\lambda \geq 0$.*

Proof. Throughout the proof, let $x, y \in \Delta_{m-1}^n$ such that $x \neq y$ and define the index sets

$$S^+ := \{i \mid x_i > y_i\} \quad \text{and} \quad S^- := \{j \mid x_j < y_j\}.$$

- a) Let $T = T^{\mathbb{P}}$ and w.l.o.g. $T(x) \geq T(y)$. Then

$$\begin{aligned} T(y) - T(x) &= -2 \log \frac{f(y)}{f(x)} = -2 \log \left(\prod_{i \in S^+} \frac{x_i!}{y_i!} \pi_i^{y_i - x_i} \cdot \prod_{j \in S^-} \frac{x_j!}{y_j!} \pi_j^{y_j - x_j} \right) \\ &= -2 \log \left(\prod_{i \in S^+} \prod_{k=1}^{x_i - y_i} \frac{y_i + k}{\pi_i} \cdot \prod_{j \in S^-} \prod_{k=1}^{y_j - x_j} \frac{\pi_j}{x_j + k} \right) \leq 0. \end{aligned}$$

Both double products contain an equal number of multiplicands (since $\sum_j x_j = \sum_j y_j = n$) and are nonempty (since $x \neq y$). As the entire product is at least 1, there exist indices $i \in S^+$ and $j \in S^-$ and natural numbers $k^+ \leq x_i - y_i$ and $k^- \leq y_j - x_j$ such that the second inequality holds in

$$\frac{\pi_j}{x_j + 1} \geq \frac{\pi_j}{x_j + k^-} \geq \frac{\pi_i}{y_i + k^+} \geq \frac{\pi_i}{x_i}.$$

Therefore, the inequality

$$T(x - e_i + e_j) = T(x) - 2 \log \left(\frac{x_i}{\pi_i} \cdot \frac{\pi_j}{x_j + 1} \right) \leq T(x)$$

holds.

- b) Let $T = T^\lambda$ and w.l.o.g. $T(x) \geq T(y)$. First, consider the case $\lambda > 0$. Note that

$$T(x) - T(y) = \frac{2}{\lambda(\lambda+1)} \left(\sum_{i \in S^+} \frac{x_i^{\lambda+1} - y_i^{\lambda+1}}{(n\pi_i)^\lambda} - \sum_{j \in S^-} \frac{y_j^{\lambda+1} - x_j^{\lambda+1}}{(n\pi_j)^\lambda} \right) \geq 0 \quad (3)$$

and

$$\begin{aligned} T(x - e_{i^*} + e_{j^*}) &= T(x) - \frac{2}{\lambda(\lambda+1)} \left(\frac{x_{i^*}^{\lambda+1} - (x_{i^*} - 1)^{\lambda+1}}{(n\pi_{i^*})^\lambda} \right) \\ &\quad + \frac{2}{\lambda(\lambda+1)} \left(\frac{(x_{j^*} + 1)^{\lambda+1} - x_{j^*}^{\lambda+1}}{(n\pi_{j^*})^\lambda} \right) \end{aligned} \quad (4)$$

for $i^* \in S^+, j^* \in S^-$. If

$$i^* = \arg \max_{i \in S^+} \frac{x_i^{\lambda+1} - (x_i - 1)^{\lambda+1}}{(n\pi_i)^\lambda}, \quad j^* = \arg \min_{j \in S^-} \frac{(x_j + 1)^{\lambda+1} - x_j^{\lambda+1}}{(n\pi_j)^\lambda}$$

and $d = d(x, y)$, then

$$\begin{aligned} \frac{x_{i^*}^{\lambda+1} - (x_{i^*} - 1)^{\lambda+1}}{(n\pi_{i^*})^\lambda} &= \frac{1}{d} \sum_{i \in S^+} \sum_{k=1}^{x_i - y_i} \frac{x_{i^*}^{\lambda+1} - (x_{i^*} - 1)^{\lambda+1}}{(n\pi_{i^*})^\lambda} \\ &\geq \frac{1}{d} \sum_{i \in S^+} \sum_{k=1}^{x_i - y_i} \frac{x_i^{\lambda+1} - (x_i - 1)^{\lambda+1}}{(n\pi_i)^\lambda} \\ &\geq \frac{1}{d} \sum_{i \in S^+} \sum_{k=1}^{x_i - y_i} \frac{(x_i + 1 - k)^{\lambda+1} - (x_i - k)^{\lambda+1}}{(n\pi_i)^\lambda} \\ &= \frac{1}{d} \sum_{i \in S^+} \frac{x_i^{\lambda+1} - y_i^{\lambda+1}}{(n\pi_i)^\lambda} \\ &\stackrel{(3)}{\geq} \frac{1}{d} \sum_{j \in S^-} \frac{y_j^{\lambda+1} - x_j^{\lambda+1}}{(n\pi_j)^\lambda} \quad (5) \\ &= \frac{1}{d} \sum_{j \in S^-} \sum_{k=1}^{y_j - x_j} \frac{(x_j + k)^{\lambda+1} - (x_j - 1 + k)^{\lambda+1}}{(n\pi_j)^\lambda} \\ &\geq \frac{1}{d} \sum_{j \in S^-} \sum_{k=1}^{y_j - x_j} \frac{(x_j + 1)^{\lambda+1} - x_j^{\lambda+1}}{(n\pi_j)^\lambda} \\ &\geq \frac{1}{d} \sum_{j \in S^-} \sum_{k=1}^{y_j - x_j} \frac{(x_{j^*} + 1)^{\lambda+1} - x_{j^*}^{\lambda+1}}{(n\pi_{j^*})^\lambda} \end{aligned}$$

$$= \frac{(x_{j^*} + 1)^{\lambda+1} - x_{j^*}^{\lambda+1}}{(n\pi_{j^*})^\lambda},$$

Hence, $T(x) \geq T(x - e_{i^*} + e_{j^*})$ by equation (4).

For $\lambda = 0$, simply taking the limit (as $\lambda \rightarrow 0$) in the above equations with

$$\begin{aligned} i^* &= \arg \max_{i \in S^+} 2x_i \log \left(\frac{x_i}{n\pi_i} \right) - 2(x_i - 1) \log \left(\frac{x_i - 1}{n\pi_i} \right), \\ j^* &= \arg \min_{j \in S^-} 2(x_j + 1) \log \left(\frac{x_j + 1}{n\pi_j} \right) - 2x_j \log \left(\frac{x_j}{n\pi_j} \right). \end{aligned}$$

yields the desired inequality, since

$$\begin{aligned} & 2x_{i^*} \log \left(\frac{x_{i^*}}{n\pi_{i^*}} \right) - 2(x_{i^*} - 1) \log \left(\frac{x_{i^*} - 1}{n\pi_{i^*}} \right) \\ &= \lim_{\lambda \rightarrow 0} \frac{2}{\lambda(\lambda + 1)} x_{i^*} \left(\left(\frac{x_{i^*}}{n\pi_{i^*}} \right)^\lambda - 1 \right) \\ &\quad - \lim_{\lambda \rightarrow 0} \frac{2}{\lambda(\lambda + 1)} (x_{i^*} - 1) \left(\left(\frac{x_{i^*} - 1}{n\pi_{i^*}} \right)^\lambda - 1 \right) \\ &= \lim_{\lambda \rightarrow 0} \frac{2}{\lambda(\lambda + 1)} \left(\frac{x_{i^*}^{\lambda+1} - (x_{i^*} - 1)^{\lambda+1}}{(n\pi_{i^*})^\lambda} - 1 \right) \\ &\stackrel{??}{\geq} \lim_{\lambda \rightarrow 0} \frac{2}{\lambda(\lambda + 1)} \left(\frac{(x_{j^*} + 1)^{\lambda+1} - x_{j^*}^{\lambda+1}}{(n\pi_{j^*})^\lambda} - 1 \right) \\ &= 2(x_{j^*} + 1) \log \left(\frac{x_{j^*} + 1}{n\pi_{j^*}} \right) - 2x_{j^*} \log \left(\frac{x_{j^*}}{n\pi_{j^*}} \right). \end{aligned}$$

□

The rest of this section is devoted to the proof of Theorem 3. For further details on weak quasi M-convexity and discrete convex analysis in general, see Murota (2003).

Weakly quasi M-convex functions have the important property that their sub-level sets are weakly quasi M-convex sets (Murota and Shioura, 2003, Theorem 3.10). A subset $M \subset \Delta_{m-1}^n$ is *weakly quasi M-convex* if for all distinct $x, y \in M$ there exist indices $i, j \in \{1, \dots, m\}$ such that $x_i > y_i, x_j < y_j$ and

$$x - e_i + e_j \in M \quad \text{or} \quad y + e_i - e_j \in M.$$

Equivalently, this can be characterized as follows.

Lemma 5. *A subset $M \subset \Delta_{m-1}^n$ is weakly quasi M-convex if and only if for all $x, y \in M$ and $d = d(x, y)$ there exists a sequence $x_0, x_1, \dots, x_d \in M$ with $x_0 = x, x_d = y$ and $d(x_i, x_{i+1}) = 1$ for all $i = 0, 1, \dots, d - 1$.*

Proof.

“ \Rightarrow ”: By induction on d : Let $x, y \in M$ and $d = d(x, y)$. If $d = 0$, then $x = x_0 = y$ satisfies the condition. If $d > 0$, define $x_{d-1} = y + e_i - e_j$ for some i, j such that $x_i > y_i, x_j < y_j$ and w.l.o.g. $x_{d-1} \in M$. Then $d(x_{d-1}, y) = 1$ and

$$\begin{aligned} d(x, x_{d-1}) &= \frac{1}{2} \left(\sum_{k \neq i, j} |x_k - y_k| + \underbrace{|x_i - (y_i + 1)|}_{=|x_i - y_i| - 1} + \underbrace{|x_j - (y_j - 1)|}_{=|x_j - y_j| - 1} \right) \\ &= \frac{1}{2} (\|x - y\|_1 - 2) = d - 1. \end{aligned}$$

By induction hypothesis, there exists a sequence $x_0, x_1, \dots, x_{d-1} \in M$ such that, $x = x_0, x_1, \dots, x_{d-1}, x_d = y \in M$ is the sought-after sequence.

“ \Leftarrow ”: Let $x, y \in M$ and $d = d(x, y)$. Let x_0, x_1, \dots, x_d be a sequence as in the lemma. As $d(x, x_1) = 1$, there exist i, j such that $x_1 = x - e_i + e_j$. Furthermore, $x_i > y_i$ and $x_j < y_j$, since

$$\begin{aligned} d - 1 &= \sum_{l=1}^{d-1} d(x_l, x_{l+1}) \\ &\geq d(x_1, y) = \frac{1}{2} \left(\sum_{k \neq i, j} |x_k - y_k| + |x_i - 1 - y_i| + |x_j + 1 - y_j| \right). \end{aligned} \quad \square$$

With this, the theorem can be proven as follows.

Proof of Theorem 3. Let t be minimal such that $A = \{x \in B_r(y) \mid T(x) \leq t\}$ has probability mass $\sum_{x \in A} f(x) \geq 1 - \alpha$ and $A \cap (B_r(y) \setminus B_{r-1}(y)) = \emptyset$ (i.e., $A \subseteq B_{r-1}(y)$). Furthermore, fix $a \in A$ such that $T(a) = t$.

Assume there exists some $b \in A_{n,\pi}^T(\alpha) \setminus A$, i.e., $T(b) \leq t$ and $b \notin B_r(y)$. Recall that the test statistic T is weakly quasi M-convex and therefore the sublevel set $L = \{x \in \Delta_{m-1}^n \mid T(x) \leq t\}$ is weakly quasi M-convex. By Lemma 5, there exists a sequence $a = a_0, a_1, \dots, a_d = b \in L$ with $d = d(a, b)$ and $d(a_i, a_{i+1}) = 1$ for all $i = 0, 1, \dots, d-1$. By the triangle inequality $d(a_i, y) - 1 \leq d(a_{i+1}, y) \leq d(a_i, y) + 1$. Thus, there exists some $j \in \{1, \dots, d-1\}$ such that $d(a_j, x) = r$, a contradiction (as $T(a_j) \leq t$ and $a_j \in B_r(y) \setminus B_{r-1}(y)$). Therefore, $A_{n,\pi}^T(\alpha) \subseteq A$ and, hence, $A = A_{n,\pi}^T(\alpha)$. \square

3.2. Calculating a p -value

As described in the previous subsection, an acceptance region can be determined by starting at some arbitrary point and increasing the radius of a ball around this point until the acceptance region is found using the criterion provided by Theorem 3. Obviously, a point that is not within the acceptance region is not a practical starting point and, ideally, one would like to start at the center of the acceptance region, to minimize the necessary iterations and number of points for which to evaluate the pmf and the test statistic. The expected value $\mathbb{E}X = n \cdot p$

of the multinomial distribution, which is the center of mass of all probability weighted points in the discrete simplex, is known and must be close to the center of mass of the acceptance region, as the acceptance region contains most of the mass. Therefore, a sample point close to the expected value should serve as a good starting point.

The p -value of an observation x can be found by calculating the total probability of the largest acceptance region not containing the observation. Though, this region can be large if the p -value of the observation is very small. To avoid this, Algorithm 1 does not calculate very small p -values precisely, but only determines precise p -values above a certain threshold θ and otherwise states that the p -value is smaller than the threshold θ . Figure 5 illustrates the points evaluated by Algorithm 1 for samples with p -value greater, respectively smaller than some threshold θ .

Algorithm 1 Calculate exact p -value above some threshold.

Require: Observation $x \in \Delta_{m-1}^n$, hypothesis $\pi \in \Delta_{m-1}$, threshold $0 < \theta \ll 1$

Ensure: Exact p -value $p \in [\theta, 1]$ or 0 if the p -value is less than θ .

Calculate $y \in \Delta_{m-1}^n$ minimizing $d(y, \mathbb{E}_\pi X)$

if $T(x) \leq T(y)$ **then**

Set $y = x$

end if

Initialize $r = 1$, SumProb = 0

repeat

Add $f(z)$ to SumProb for points $z \in B_r(x) \setminus B_{r-1}(y)$ with $T(z) < T(x)$

Increment $r = r + 1$

until $T(x) \leq \min\{T(z) \mid d(y, z) = r\}$ **or** SumProb $> 1 - \theta$

if SumProb $\leq 1 - \theta$ **then**

return $1 - \text{SumProb}$

else

return 0

end if

3.3. Implementation

Enumeration of the full sample space can be implemented using a simple recursion. A similar, more complicated recursive scheme can be employed to enumerate the samples at a given radius r in the repeat-loop of Algorithm 1. This is implemented in the R package **ExactMultinom** using a C++ subroutine to allow for fast recursions.

As mentioned in the introduction, algorithms for calculating exact multinomial tests superior to the full enumeration method have been proposed in the literature. However, readily available open source implementations of these methods apparently do not exist. There are two packages implementing exact multinomial tests using full enumeration of the sample space in R, namely, EMT (Menzel, 2013) and XNomial (Engels, 2015). Whereas EMT is written purely in R, the function `xmulti` of the XNomial package implements the full enumeration method using an efficient C++ subroutine for the recursion, which makes it a lot more efficient. Therefore, `xmulti` was selected as reference method.

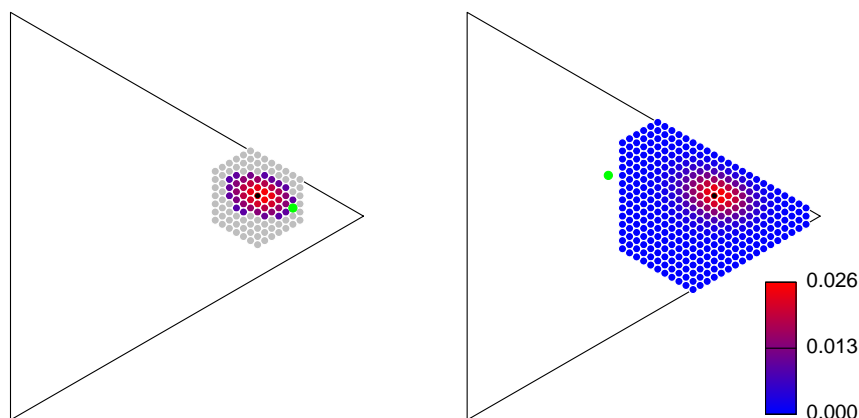


FIG 5. Samples in $\Delta_2(50)$ for which the probability mass and test statistic are evaluated given the green observations $x = (4, 40, 6)$ (left) and $x = (10, 20, 20)$ (right) under the null hypothesis $p = (\frac{1}{10}, \frac{7}{10}, \frac{2}{10})$ and $T = T^{\mathbb{P}}$. The p -values are 0.3049 (left) and less than $\theta = 0.0001$ (right). The colored region on the left indicates the smallest acceptance region not containing the observed sample. The color gradient represents (null) probabilities within the regions.

In the implementation of Algorithm 1 the p -values for the chi-square, log-likelihood ratio and probability mass test statistics are computed simultaneously, as in `xmulti` and so comparability is ensured.

The current implementation of Algorithm 1 accurately finds p -values of order roughly as small as 10^{-10} . Smaller p -values will often lead to negative output because of limited computational precision in the addition of many floating point numbers. To ensure accurate results, I recommend to choose θ no less than 10^{-8} with the current implementation.

During early runs of the simulation study described in Section 4, it was noticed that the runtime of Algorithm 1 tends to increase drastically if the null distribution contains very small probabilities, that is, there exists some i with $\pi_i \ll n^{-1}$. This is due to the acceptance regions becoming very flat and containing mostly points within a lower dimensional face of the discrete simplex for such null hypotheses. In this case, n is too small for Proposition 6 below to take effect. As a heuristic, which turned out to be an effective remedy, the implementation does not enumerate entire balls if $n \cdot \pi_i < \frac{1}{2}$, but only considers points $z \in \Delta_{m-1}^n$ with small z_i , by skipping all points z for which $\mathbb{P}_\pi(X_i \geq z_i) < \theta \cdot 10^{-8}$.

3.4. Runtime complexity

The discrete simplex Δ_{m-1}^n contains $|\Delta_{m-1}^n| = \binom{n+m-1}{m-1}$ points and so the full enumeration takes $\mathcal{O}(n^{m-1})$ operations to compute a p -value. In comparison,

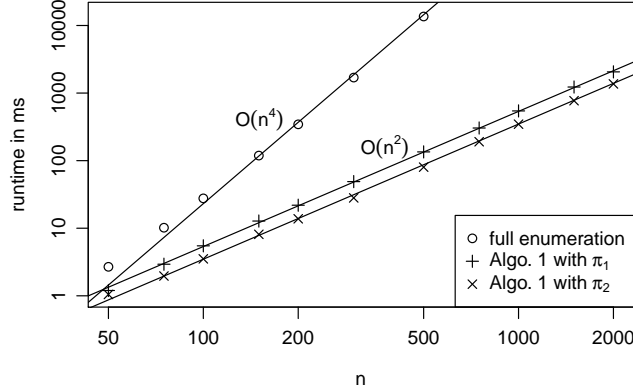


FIG 6. Runtime of the full enumeration method and Algorithm 1 when enumerating a ball with probability mass $1 - \theta$ for $\theta = 0.0001$ and null hypotheses $\pi_1 = (0.2, 0.2, 0.2, 0.2, 0.2)$, respectively $\pi_2 = (0.01, 0.19, 0.2, 0.3, 0.3)$. If the p -values of an observation are significantly larger than θ , the runtime of Algorithm 1 considerably decreases. Times are mean values from 10 runs.

the acceptance regions at a fixed level $\alpha > 0$ only contain $\mathcal{O}(n^{\frac{m-1}{2}})$ points and this continues to hold for the smallest ball centered at the expected value containing the acceptance region, as proven by Proposition 6 below. Therefore, Algorithm 1 only takes $\mathcal{O}(n^{\frac{m-1}{2}})$ operations to determine a p -value above the threshold θ . Figure 6 shows runtime as a function of n for $m = 5$. Whereas the runtime of the full enumeration method does not depend on the choice of π and the observation x , the runtime of Algorithm 1 increases if the p -value of x is small. Furthermore, the choice of π also influences the runtime of Algorithm 1 with the uniform null hypothesis resulting in a longer runtime than sparse null hypotheses. This is further investigated in the simulation study in Section 4. As the runtime increases exponentially in m , Algorithm 1 is only feasible if the number of categories m is small.

Proposition 6. For $T \in \{T^{\chi^2}, T^G, T^{\mathbb{P}}\}$, there exists c such that $A^T(\alpha) \subset B_{\sqrt{nc}}(n\pi)$ for sufficiently large n .

Proof. Consider the canonical extension \bar{T} of T to $\bar{\Delta}_{m-1}^n = \{x \in \mathbb{R}_{\geq 0}^m : x_1 + \dots + x_m = n\}$ and let $B_r(n\pi) = \{x \in \bar{\Delta}_{m-1}^n : \frac{1}{2}\|x - n\pi\|_1 \leq r\}$ a ball in $\bar{\Delta}_{m-1}^n$ with boundary $\partial B_r(n\pi) = \{x \in \bar{\Delta}_{m-1}^n : \frac{1}{2}\|x - n\pi\|_1 = r\}$. Let $r_0 = \min_j \pi_j > 0$ and $n_0 \in \mathbb{N}$. If $n \geq n_0$, then every $x \in \partial B_{\sqrt{nn_0}r_0}(n\pi)$ can be written as $x = x(n, x_0) := n\pi + \sqrt{nn_0}(x_0 - \pi)$ for some $x_0 \in \partial B_{r_0}(\pi)$.

Let $(t_{n,1-\alpha})$ be the sequence of $(1 - \alpha)$ -quantiles of $T_n = T(X_n)$, $X_n \sim \mathcal{M}_m(n, \pi)$ for $n \in \mathbb{N}$. As T_n converges to χ_{m-1}^2 in distribution, the sequence of quantiles converges to the $(1 - \alpha)$ -quantile $\chi_{m-1,1-\alpha}^2$ (cf. Van der Vaart, 1998, Lemma 21.2). Consequently, the maximum $t = \max_n t_{n,1-\alpha}$ exists and the set $A_n = \{x \in \bar{\Delta}_{m-1}^n : \bar{T}(x) \leq t\}$ contains the acceptance region $A_n^T(\alpha)$ for every n .

As \bar{T} is convex (Lemma 8 in Appendix B) and thus has convex sublevel

sets, it suffices to show that n_0 can be chosen such that $\min_{x \in \partial B_{\sqrt{nn_0}r_0}(n\pi)} \bar{T}(x)$ converges to a value $> t$ to ensure that $A_n^T(\alpha) \subset A_n \subset B_{\sqrt{n}(\sqrt{n_0}r_0)}(n\pi)$ for sufficiently large n .

In case $T = T^{\chi^2}$, observe that

$$\bar{T}(x(n, x_0)) = \sum_j \frac{(x_j(n, x_0) - n\pi_j)^2}{n\pi_j} = \sum_j \frac{n_0(x_{0,j} - \pi_j)^2}{\pi_j}$$

does not depend on n and so the canonical extension \bar{T} of the chi-square statistic at radius $\sqrt{nn_0}r_0$ is bounded from below by $b(n_0) = \min_{x \in \partial B_{r_0}(n_0\pi)} \bar{T}(x)$. This bound becomes arbitrarily large as n_0 is increased.

In case $T = T^G$ or $T = T^{\mathbb{P}}$, if n_0 is fixed, $\bar{T}(x(n, x_0))$ converges uniformly to $\bar{T}^{\chi^2}(x(n, x_0))$ for $x_0 \in \partial B_{r_0}(\pi)$ (Lemma 9 in Appendix B). Therefore, the minimum $\min_{x \in \partial B_{\sqrt{nn_0}r_0}(n\pi)} \bar{T}(x)$ converges to $b(n_0)$. \square

4. Application

In this section, the use of the new method is illustrated in a simulation study. On the one hand, this serves to show the improvements in runtime in comparison to the full enumeration method. On the other hand, this sheds some light on the fit of the asymptotic approximation to the probability mass test provided by Theorem 1 for a medium sample size ($n = 100$).

As a practical application, the usage of exact multinomial tests to increase the information conveyed by the *calibration simplex* (Wilks, 2013), a graphical tool used to assess ternary probability forecasts, is outlined.

4.1. Simulation study

For the simulation study, pairs $(\pi^{(1)}, x^{(1)}), \dots, (\pi^{(N)}, x^{(N)})$ of null hypothesis parameters and samples were generated as i.i.d. realizations of the random quantity (P, X) with $P \sim \mathcal{U}(\Delta_{m-1})$ being uniformly distributed on the unit simplex and $X \mid P \sim \mathcal{M}_m(n, P)$. Then, for each pair, p -values were computed using various test statistics and algorithms. In this way, no specific null hypothesis has to be chosen and instead a wide variety is considered. By drawing samples from the null hypotheses, p -values follow a uniform distribution on $[0, 1]$. Various aspects of the tests and algorithms in question can be examined using the resulting rich data set and subsets thereof.

The following results were obtained using $N = 10^6$ such pairs with samples of size $n = 100$ drawn from multinomial distributions with $m = 5$ outcomes. Exact p -values were computed using the implementation of Algorithm 1 provided by the accompanying R package for all pairs. To estimate the speedup achieved by the new method in this study, the full enumeration method provided by the `xmulti` function of the `XNomial` package (Engels, 2015) was applied to the first 10^4 pairs. Essentially, the computational cost of the full enumeration is constant, independent of the null hypothesis at hand and the resulting p -value, whereas

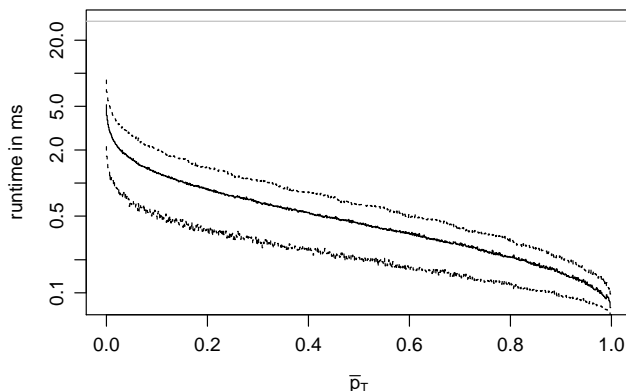


FIG 7. Runtime against mean p -value in groups of 1000 samples with similar mean p -value. The solid line shows mean runtime per group, whereas the dashed lines are the 5% and 95%-quantile. The gray line shows the mean runtime using full enumeration.

the cost of Algorithm 1 increases as the p -value decreases and also varies with the null hypothesis.

The implementation of Algorithm 1 took an average of 0.59 ms to calculate a p -value, whereas the full enumeration took 29.76 ms on average and so execution of the new method was about 50 times as fast. Perhaps surprisingly, Monte Carlo estimation (using `xmonte` from `XNomial`, which simulates 10000 samples by default) took almost twice as long (53.49 ms) as the full enumeration. Figure 7 illustrates the connection between runtime and size of the resulting p -values for the new method. As there are other factors influencing the runtime and, as described in the previous section, the implementation computes p -values for multiple statistics simultaneously, samples were ordered by their mean p -value $\bar{p}_T = \frac{1}{3}(p_{T^P} + p_{T^{\chi^2}} + p_{T^G})$ and then put in groups of 1000 samples each with similar mean p -value (in particular, a group contains all samples in between the empirical α - and $(\frac{\alpha+1}{1000})$ -quantile for $\alpha = \frac{a}{1000}$ and $a = 0, \dots, 999$). The figure shows mean runtime in each group as well as the 5%- and 95%-quantile.

To illustrate the fit of the classical chi-square approximation, the probability of a chi-square distribution with $m - 1$ degrees of freedom exceeding the values of the test statistics for each pair were computed. Figure 8 shows relative errors of the asymptotic approximations to the p -values for the three test statistics. Given a test statistic T and asymptotic approximation $\tilde{p}_T = \tilde{p}_T(x, \pi)$ to the exact p -value $p_T = p_T(x, \pi)$, the relative error was calculated as $\frac{\tilde{p}_T - p_T}{p_T}$, that is, the deviation of the approximation from the exact value in parts of the exact value. It can be seen that the asymptotic approximation to the chi-square statistic is quite accurate in most cases, but tends to underestimate small p -values (< 0.1). The asymptotic approximation to the log-likelihood ratio statistic tends to slightly underestimate p -values on average. Asymptotic approximations of

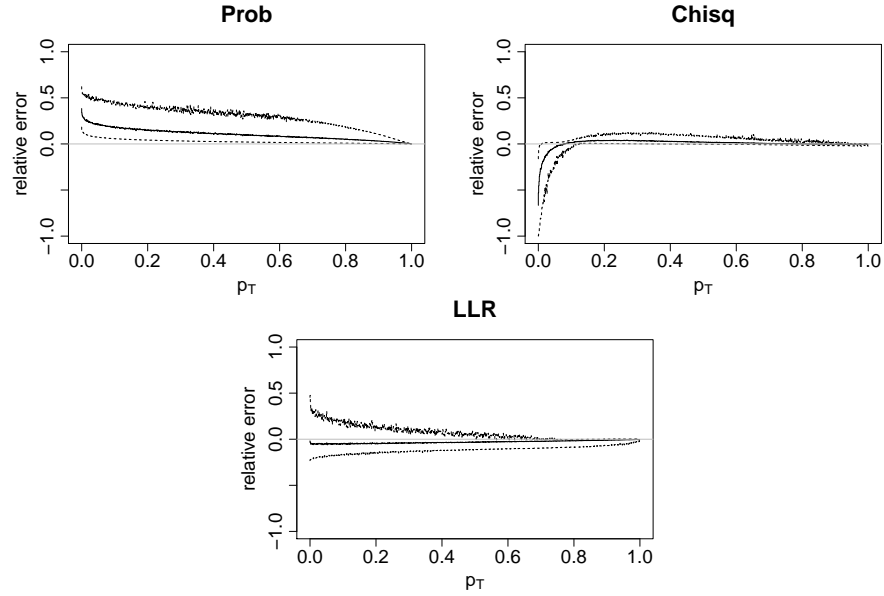


FIG 8. Relative errors of asymptotic approximation for probability mass (*Prob*), chi-square (*Chisq*) and log-likelihood ratio (*LLR*) test statistic. The plots were obtained using the same grouping scheme as in Figure 7.

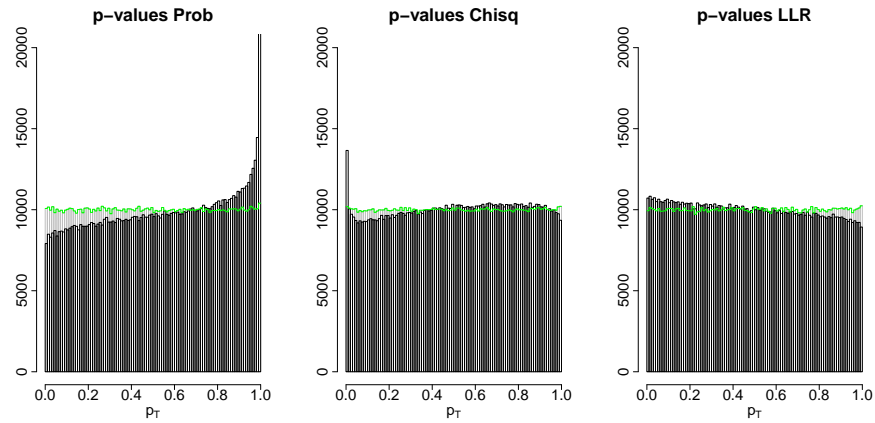


FIG 9. Histograms of asymptotic approximations to p -value for probability mass (*Prob*), chi-square (*Chisq*) and log-likelihood ratio (*LLR*) test statistic in black. The green lines indicate histograms of respective exact p -values. The rightmost bar within the left histogram is not fully shown and extends further up to over 30000 counts.

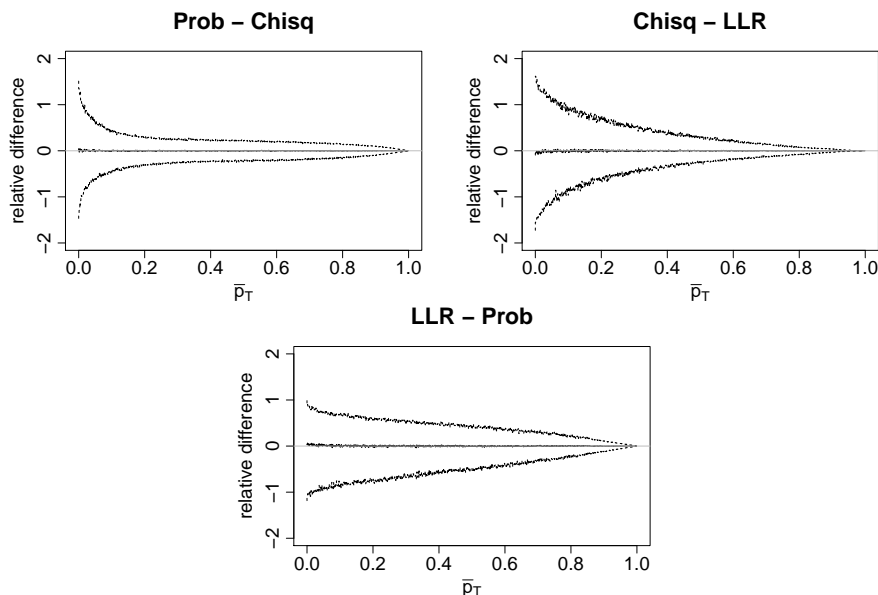


FIG 10. Relative differences between exact p -values of probability mass (Prob), chi-square (Chisq) and log-likelihood ratio (LLR) test statistic against mean of compared p -values. The plots were obtained using the same grouping scheme as in Figure 7.

Pearson's chi-square and the log-likelihood ratio have been studied well and the classical chi-square approximations can be improved by using moment corrections (see [Cressie and Read, 1989](#), and references therein). Furthermore, the errors typically increase if some category has small expectation under the null hypothesis. It can be seen that the approximation to the probability mass p -values provided by Theorem 1 produces somewhat larger errors especially for large p -values and that it clearly overestimates the p -values. This is emphasized by the fact that within the simulation data only a vanishingly small number of p -values was slightly underestimated, all of which were well over 0.9. Figure 9 illustrates how these estimation errors influence the distribution of the resulting p -values. Whereas the exact p -values clearly follow a uniform distribution (indicated in green), the asymptotic p -values clearly deviate from uniformity. For the probability mass statistic, the asymptotic test clearly yields a conservative test, whereas the asymptotic log-likelihood ratio test (and also the asymptotic chi-square test at small significance levels) is slightly anti-conservative.

Lastly, Figure 10 shows relative differences between exact p -values obtained with the three test statistics. Given test statistics T and T' , the relative difference between p -values $p_T = p_T(x, \pi)$ and $p_{T'} = p_{T'}(x, \pi)$ is calculated as $\frac{p_T - p_{T'}}{\bar{p}_T}$ with $\bar{p}_T = \frac{p_T + p_{T'}}{2}$. It can be seen that the choice of test statistic can make quite a difference. A closer look at the simulation data revealed that these differences tend to be smaller if expectations for all categories are large under the null. To

TABLE 1
Exact p -values p_T and asymptotic p -values \tilde{p}_T of five randomly selected pairs (x, π) with $0.01 < p_{TG}(x, \pi) < 0.1$.

| π | $p_{T^{\mathbb{P}}}$ | $\tilde{p}_{T^{\mathbb{P}}}$ | $p_{T\chi^2}$ | $\tilde{p}_{T\chi^2}$ | p_{TG} | \tilde{p}_{TG} |
|-------------------------------------|----------------------|------------------------------|---------------|-----------------------|----------|------------------|
| (0.116, 0.225, 0.259, 0.002, 0.398) | 0.0068 | 0.0092 | 0.0190 | 0.0073 | 0.0126 | 0.0172 |
| (0.038, 0.079, 0.224, 0.387, 0.272) | 0.1150 | 0.1268 | 0.1437 | 0.1469 | 0.0361 | 0.0307 |
| (0.595, 0.129, 0.093, 0.064, 0.118) | 0.0447 | 0.0495 | 0.0477 | 0.0482 | 0.0719 | 0.0665 |
| (0.497, 0.217, 0.223, 0.057, 0.007) | 0.0761 | 0.0994 | 0.0803 | 0.0741 | 0.0461 | 0.0498 |
| (0.243, 0.022, 0.237, 0.373, 0.125) | 0.0474 | 0.0566 | 0.0508 | 0.0507 | 0.0628 | 0.0568 |

provide some numerical insights, Table 1 lists exact and asymptotic p -values.

4.2. The calibration simplex

Turning to an application in forecast verification, consider a random variable X and a probabilistic forecast F for X . For an introduction to probabilistic forecasting in general, see [Gneiting and Katzfuss \(2014\)](#). A probabilistic forecast is said to be *calibrated* if the conditional distribution of the quantity of interest given a forecast coincides with the forecast distribution, that is,

$$X \mid F \sim F \quad (6)$$

holds almost surely. Suppose now that X maps to one of three distinct outcomes only. Then, a probabilistic forecast is fully described by the probabilities it assigns to each outcome.

In this case, the calibration simplex ([Wilks, 2013](#)) can be used to graphically identify discrepancies in predicted probabilities and conditional outcome frequencies. Given i.i.d. realizations $(f_1, x_1), \dots, (f_N, x_N)$ consisting of forecast probabilities (vectors within the unit 2-simplex) and observed outcomes encoded 1, 2 and 3, forecast-outcome pairs with similar forecast probabilities are grouped according to a tessellation of the probability simplex. Thereafter, calibration is assessed by comparing average forecast and actual outcome frequencies within each group.

As illustrated in Figure 11, the calibration simplex is a graphical tool, to conduct this comparison visually. The groups are determined by overlaying the probability simplex with a hexagonal grid. The circular dots correspond to nonempty groups of forecasts given by a hexagon. The dots' areas are proportional to the number of forecasts per group. A dot is shifted away from the center of the respective hexagon by a scaled version of the difference in average forecast probabilities and outcome frequencies. This provides valuable insight into the forecast's distribution and the conditional distribution of the quantity of interest. However, it is not apparent how big the differences may be merely by chance.

If the forecast is calibrated, then, by (6), the outcome frequencies \bar{x} within a group of size n with mean forecast \bar{f} follow a generalized multinomial distribution (the multinomial analog of the Poisson binomial distribution), that is, a convolution of multinomial distributions $\mathcal{M}(1, f_i)$ with parameters $f_1, \dots, f_n \in$

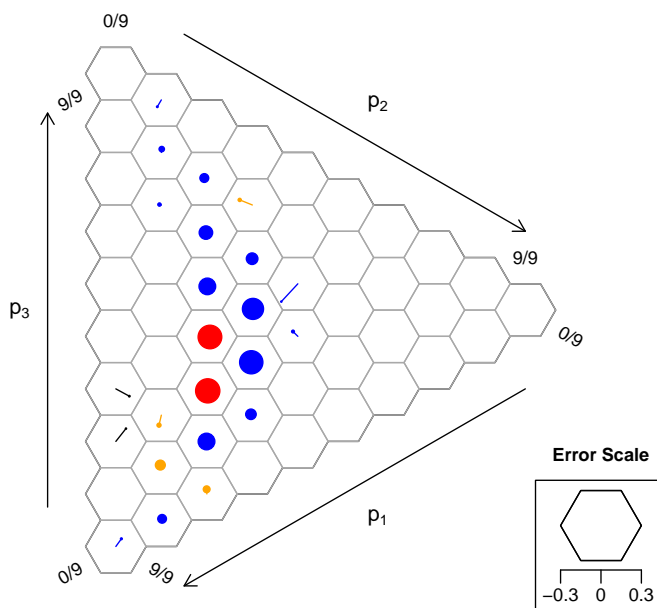


FIG 11. Calibration Simplex with color-coded p -values using the probability mass statistic. This example evaluates a total of 21240 club soccer predictions by FiveThirtyEight (<https://projects.fivethirtyeight.com/soccer-predictions/>) for matches from September 2016 until April 2019. Outcomes are encoded as 1 = “home win”, 2 = “draw” and 3 = “away win”. Only groups containing at least ten forecasts are shown. Blue indicates a p -value $p_{TG} \geq 0.1$, orange $0.1 > p_{TG} \geq 0.01$, red $p_{TG} < 0.01$ and black $p_{TG} = 0$.

Δ_{m-1} . If these parameters only deviate little from their mean $\bar{f} = \frac{1}{n} \sum_i f_i$, then, presumably, the generalized multinomial distribution should not deviate much from a multinomial distribution with parameter \bar{f} . Under this presumption, multinomial tests can be applied to quantify the discrepancy within each group through a p -value. As the number of outcomes $m = 3$ is small, exact p -values are efficiently computed by Algorithm 1 even for large sample sizes n .

In Figure 11 p -values obtained from the log-likelihood ratio statistic are conveyed through a coloring scheme. Note that a p -value will only ever be exactly zero, if an outcome is forecast to have zero probability and said outcome still realizes. Figure 11 was generated using the R package CalSim (Resin, 2020).

The calibration simplex can be seen as a generalization of the popular reliability diagram. In light of this analogy, the use of multinomial tests to assess the statistical significance of differences in predicted probabilities and observed outcome frequencies serves the same purpose as consistency bars in reliability diagrams introduced by Bröcker and Smith (2007). Consistency bars are constructed using Monte Carlo simulation. To justify the above presumption, the multinomial p -values used to construct Figure 11 were compared to p -values calculated from 10000 Monte Carlo samples obtained from the generalized multi-

nomial distributions. To this end, the standard deviation of the Monte Carlo p -values was estimated using the estimated p -value in place of the true generalized multinomial p -value. Most of the multinomial p -values were quite close to the Monte Carlo estimates with an absolute difference less than two standard deviations, whereas two of them deviated on the order of 6 to 8 standard deviations from the Monte Carlo estimates, which nonetheless resulted in a relatively small absolute error. In particular, using the Monte Carlo estimated p -values did not change Figure 11. As computation of the Monte Carlo estimates from the generalized multinomial distributions is computationally expensive, the multinomial p -values serve as a fast and adequate alternative. Further improving uncertainty quantification within the calibration simplex is a subject for future work.

5. Concluding Remarks

A new method for calculating exact p -values was investigated. It has been illustrated that the new method works well when the number m of categories is small. This results in a concrete speedup in practical applications as illustrated through a simulation study.

Regarding the choice of test statistic, the “exact multinomial test” was treated as a test statistic and the asymptotic distribution of the resulting probability mass statistic was derived. Like most prominent test statistics, the probability mass statistic yields unbiased tests for the uniform null hypothesis. It was shown that a randomized test based on the probability mass statistic can be characterized in that it minimizes the respective (weighted) acceptance region.

Although asymptotic approximations work well in many use cases, there are cases, where these approximations are not adequate, for example, when dealing with small sample sizes or small expectations. On the other hand, there is nothing to be said against the use of exact tests whenever feasible and it is recommended in the applied literature (McDonald, 2009, p. 83) for samples of moderate size up to 1000. As the available implementations of exact multinomial tests in R use full enumeration, the new implementation increases the scope of exact multinomial tests for practitioners.

Appendix A: Difference Between Log-Likelihood Ratio and Probability Mass Statistic

Lemma 7. *Let $\pi \in \Delta_{m-1}$ with $\pi_j > 0$ for all $j = 1, \dots, m$ and $x \in \Delta_{m-1}^n$. Then*

$$T^{\mathbb{P}}(x, \pi) - T^G(x, \pi) = \sum_{j=1}^m (\log(x_j) + 2r(x_j) - \log(n\pi_j) - 2r(n\pi_j))$$

for a function r on the positive real numbers for which $0 < r(x) < \frac{1}{12x}$ for $x > 0$. In case $x_j = 0$ for some $j = 1, \dots, m$, the above equality holds if $\log(0) + 2r(0)$ is understood to be 0.

Proof. The logarithm of the Gamma function can be written as

$$\log \Gamma(x+1) = \log x \Gamma(x) = x \log(x) - x + \frac{1}{2} \log(2\tilde{\pi}x) + r(x)$$

for a function r on the positive real numbers for which $0 < r(x) < \frac{1}{12x}$ holds for all $x > 0$ (see [Abramowitz and Stegun, 1972](#), 6.1.41 and 6.1.42; here $\tilde{\pi}$ denotes Archimedes' constant). This yields

$$\begin{aligned} \log \bar{f}_{n, \frac{y}{n}}(y) &= \log \Gamma(n+1) + \sum_j \left(y_j \log \frac{y_j}{n} - \log \Gamma(y_j+1) \right) \\ &= \log \Gamma(n+1) + \sum_j \left(y_j \log \frac{y_j}{n} - y_j \log(y_j) + y_j - \frac{1}{2} \log(2\tilde{\pi}y_j) - r(y_j) \right) \\ &= \log \Gamma(n+1) + n(1 - \log n) - \sum_j \left(\frac{1}{2} \log(2\tilde{\pi}y_j) + r(y_j) \right) \end{aligned}$$

for $y \in \mathbb{R}_{>0}^m$ such that $\sum_j y_j = n$, and hence

$$\begin{aligned} T^{\mathbb{P}}(x, \pi) - T^G(x, \pi) &= 2(\log \bar{f}_{n, \pi}(n\pi) - \log f_{n, \frac{x}{n}}(x)) \\ &= 2 \sum_j \left(\frac{1}{2} \log \frac{x_j}{n\pi_j} + r(x_j) - r(n\pi_j) \right) \end{aligned}$$

□

Appendix B: Details for the Proof of Proposition 6

The following two lemmas provide further details not contained in the proof of Proposition 6 itself.

Lemma 8. *Using notation as in the proof of Proposition 6, $x \mapsto \bar{T}(x)$ is convex.*

Proof. The function $x \mapsto \bar{T}^{x^2}(x) = \sum_j \frac{x_j^2}{n\pi_j} - n$ is clearly convex as it is a sum of convex functions.

The function $x \mapsto \bar{T}^G(x) = 2 \sum_j x_j \log(x_j) - x_j \log(n\pi_j)$ is convex since $x \mapsto x \log(x)$ is convex (an elementary proof of this can be given using either the inequality of the arithmetic and geometric means or the second derivative).

The function $x \mapsto \bar{T}^{\mathbb{P}}(x) = 2(\log(\bar{f}_{n, \pi}(n\pi)) - \log(\Gamma(n+1)) + \sum_j \log(\Gamma(x_j+1)) - \sum_j x_j \log(\pi_j))$ is convex as the Gamma function is logarithmically convex by the Bohr-Mollerup theorem ([Beals and Wong, 2010](#), Theorem 2.4.2). □

Lemma 9. *Using notation as in the proof of Proposition 6, the function $\partial B_{r_0}(\pi) \rightarrow \mathbb{R}, x_0 \mapsto \bar{T}(x(n, x_0))$ converges uniformly to $\bar{T}^{x^2}(x(n, x_0))$ as $n \rightarrow \infty$ if $T = T^G$ or $T = T^{\mathbb{P}}$.*

Proof. Let $x_0 \in \partial B_{r_0}(\pi)$ and define $c = c(x_0) := \sqrt{n_0}(x_0 - \pi)$. Hence $|c_j| \leq \sqrt{n_0}r_0 < \sqrt{n_0}$ for all $j = 1, \dots, m$. Consider first the case $T = T^G$. Then (using the Taylor expansion $\log(1+x) = \sum_{k=1}^{\infty} (-1)^{k+1} \frac{x^k}{k}$)

$$\begin{aligned} \bar{T}(x(n, x_0)) &= 2 \sum_{j=1}^m x(n, x_0)_j \log \frac{x(n, x_0)_j}{n\pi_j} \\ &= 2 \sum_j (n\pi_j + \sqrt{n}c_j) \log \frac{n\pi_j + \sqrt{n}c_j}{n\pi_j} \\ &= 2 \sum_j (n\pi_j + \sqrt{n}c_j) \sum_{k=1}^{\infty} \frac{(-1)^{k+1}}{k} \left(\frac{c_j}{\sqrt{n}\pi_j} \right)^k \\ &= 2 \sum_j \left(\sqrt{n}c_j + \frac{c_j^2}{2\pi_j} - \frac{c_j^3}{2\sqrt{n}\pi_j^2} + \frac{n\pi_j + \sqrt{n}c_j}{\sqrt{n}^3} \sum_{k=3}^{\infty} \frac{(-1)^{k+1} c_j^k}{k\sqrt{n}^{k-3}\pi_j^k} \right) \end{aligned}$$

As $\sum_j c_j = 0$ and $2 \sum_j \frac{c_j^2}{2\pi_j} = T^{\chi^2}(x(n, x_0))$, the inequalities

$$\begin{aligned} &|\bar{T}^{\chi^2}(x(n, x_0)) - \bar{T}(x(n, x_0))| \\ &< \sum_j \left(\frac{|c_j|^3}{2\sqrt{n}\pi_j^2} + \frac{n\pi_j + \sqrt{n}|c_j|}{\sqrt{n}^3} \sum_{k=3}^{\infty} \frac{|c_j|^k}{k\sqrt{n}^{k-3}\pi_j^k} \right) \\ &< \sum_j \left(\frac{\sqrt{n_0}^3}{2\sqrt{n}\pi_j^2} + \frac{n\pi_j + \sqrt{n}\sqrt{n_0}}{\sqrt{n}^3} \sum_{k=3}^{\infty} \frac{\sqrt{n_0}^k}{k\sqrt{n}^{k-3}\pi_j^k} \right) \\ &< \frac{1}{\sqrt{n}} \sum_j \left(\frac{\sqrt{n_0}^3}{2\pi_j^2} + (\pi_j + \sqrt{n_0})C(n) \right) \end{aligned}$$

hold, where the series converges to some $C(n)$ for sufficiently large n by the ratio test and $C(n)$ decreases as n increases. As this upper bound is independent of the choice of x_0 uniform convergence is ensured.

Using Lemma 7 in case $T = T^{\mathbb{P}}$, the inequality

$$\begin{aligned} &|\bar{T}^G(x(n, x_0)) - \bar{T}(x(n, x_0))| \\ &= \left| \sum_{j=1}^m \left(\log \frac{x(n, x_0)_j}{n\pi_j} + 2r(x(n, x_0)_j) - 2r(n\pi_j) \right) \right| \\ &= \left| \sum_j \left(\log \frac{n\pi_j + \sqrt{n}c_j}{n\pi_j} + 2r(n\pi_j + \sqrt{n}c_j) - 2r(n\pi_j) \right) \right| \\ &< \sum_j \left(\left| \log \left(1 - \frac{\sqrt{n_0}r_0}{\sqrt{n}\pi_j} \right) \right| + \frac{2}{12(n\pi_j - \sqrt{nn_0}r_0)} \right) \end{aligned}$$

holds and the upper bound converges to zero independent of the choice of x_0 . Hence

$$\bar{T}^{x^2} - \bar{T} = (\bar{T}^{x^2} - \bar{T}^G) + (\bar{T}^G - \bar{T})$$

converges uniformly to zero as a function on $\partial B_{r_0}(\pi)$ in the sense of the lemma. \square

References

- ABRAMOWITZ, M. and STEGUN, I. A. (1972). *Handbook of Mathematical Functions with Formulas, Graphs, and Mathematical Tables*, tenth printing ed. *National Bureau of Standards Applied Mathematics Series* **55**. Dover Publishing.
- BAGLIVO, J., OLIVIER, D. and PAGANO, M. (1992). Methods for exact goodness-of-fit tests. *Journal of the American Statistical Association* **87** 464-469.
- BEALS, R. and WONG, R. (2010). *Special Functions: A Graduate Text* **126**. Cambridge University Press.
- BEJERANO, G., FRIEDMAN, N. and TISHBY, N. (2004). Efficient exact p-value computation for small sample, sparse, and surprising categorical data. *Journal of Computational Biology* **11** 867-886.
- BRÖCKER, J. and SMITH, L. A. (2007). Increasing the reliability of reliability diagrams. *Weather and Forecasting* **22** 651-661.
- COHEN, A. and SACKROWITZ, H. B. (1975). Unbiasedness of the chi-square, likelihood ratio, and other goodness of fit tests for the equal cell case. *The Annals of Statistics* **3** 959-964.
- CRESSIE, N. and READ, T. R. C. (1984). Multinomial goodness-of-fit tests. *Journal of the Royal Statistical Society: Series B (Methodological)* **46** 440-464.
- CRESSIE, N. and READ, T. R. C. (1989). Pearson's X^2 and the loglikelihood ratio statistic G^2 : A comparative review. *International Statistical Review* **57** 19-43.
- ENGELS, B. (2015). XNomial: Exact goodness-of-fit test for multinomial data with fixed probabilities R package version 1.0.4. <https://CRAN.R-project.org/package=XNomial>.
- GIBBONS, J. D. and PRATT, J. W. (1975). P-values: Interpretation and methodology. *The American Statistician* **29** 20-25.
- GNEITING, T. and KATZFUSS, M. (2014). Probabilistic forecasting. *Annual Review of Statistics and Its Application* **1** 125-151.
- HIRJI, K. F. (1997). A comparison of algorithms for exact goodness-of-fit tests for multinomial data. *Communications in Statistics - Simulation and Computation* **26** 1197-1227.
- KEICH, U. and NAGARAJAN, N. (2006). A fast and numerically robust method for exact multinomial goodness-of-fit test. *Journal of Computational and Graphical Statistics* **15** 779-802.

- KOEHLER, K. J. and LARNTZ, K. (1980). An empirical investigation of goodness-of-fit statistics for sparse multinomials. *Journal of the American Statistical Association* 336-344.
- KOTZE, T. J. V. W. and GOKHALE, D. V. (1980). A comparison of the Pearson- χ^2 and log-likelihood-ratio statistics for small samples by means of probability ordering. *Journal of Statistical Computation and Simulation* **12** 1-13.
- LEHMANN, E. L. and ROMANO, J. P. (2005). *Testing Statistical Hypotheses*, third edition ed. *Springer Texts in Statistics*. Springer, New York.
- MCDONALD, J. H. (2009). *Handbook of Biological Statistics*, Second edition ed. Sparky House Publishing, Baltimore.
- MENZEL, U. (2013). EMT: Exact multinomial test: Goodness-of-fit test for discrete multivariate data R package version 1.1. <https://CRAN.R-project.org/package=EMT>.
- MUROTA, K. (2003). *Discrete Convex Analysis*. *SIAM Monographs on Discrete Mathematics and Applications*. Society for Industrial and Applied Mathematics (SIAM), Philadelphia, PA.
- MUROTA, K. and SHIOURA, A. (2003). Quasi M-convex and L-convex functions - quasiconvexity in discrete optimization. *Discrete Applied Mathematics* **131** 467-494.
- PÉREZ, T. and PARDO, J. A. (2003). On choosing a goodness-of-fit test for discrete multivariate data. *Kybernetes* **32** 1405-1424.
- RADLOW, R. and ALF, E. F. J. (1975). An alternate multinomial assessment of the accuracy of the χ^2 test of goodness of fit. *Journal of the American Statistical Association* **70** 811-813.
- RESIN, J. (2020). CalSim: The calibration simplex R package version 0.5.0. <https://CRAN.R-project.org/package=CalSim>.
- TATE, M. W. and HYER, L. A. (1973). Inaccuracy of the χ^2 test of goodness of fit when expected frequencies are small. *Journal of the American Statistical Association* **68** 836-841.
- R CORE TEAM (2020). R: A language and environment for statistical computing R Foundation for Statistical Computing, Vienna, Austria <https://www.R-project.org/>.
- VAN DER VAART, A. W. (1998). *Asymptotic Statistics*. *Cambridge Series in Statistical and Probabilistic Mathematics* **3**. Cambridge University Press, Cambridge.
- WAKIMOTO, K., ODAKA, Y. and KANG, L. (1987). Testing the goodness of fit of the multinomial distribution based on graphical representation. *Computational Statistics & Data Analysis* **5** 137-147.
- WEST, E. N. and KEMPTHORNE, O. (1972). A comparison of the χ^2 and likelihood ratio tests for composite alternatives. *Journal of Statistical Computation and Simulation* **1** 1-33.
- WILKS, D. S. (2013). The calibration simplex: A generalization of the reliability diagram for three-category probability forecasts. *Weather and Forecasting* **28** 1210-1218.